Sparse Phase Estimation and Processing of Independent Coherent Processing Intervals

Jabran Akhtar, Børge Torvik and Karl Erik Olsen

Norwegian Defence Research Establishment (FFI)
Box 25, 2027 Kjeller, Norway
Email: jabran.akhtar@ffi.no, borge.torvik@ffi.no, karl-erik.olsen@ffi.no

***Abstract*— Radars employing electronically steering arrays are capable of instantaneously altering the direction of the beam along with other parameters. This flexibility offers great opportunities to a radar as it may e.g. divide its time between several directions or frequently modify the waveforms being emit. These kinds of techniques can often result in several sequences of coherent processing intervals illuminating the same area, however, the data may not necessarily be coherent across the acquired sections. In this paper we propose a technique based on sparse reconstruction to transform such groups of blocks into a single continuous coherent entity. Data obtained from an experimental radar is used to validate the techniques.**

Keywords: Range-Doppler, extended dwell, coherent integration, non-coherent integration

I. Introduction

Modern pulse-Doppler radars typically engage by transmitting a number of pulses within a set coherent processing interval (CPI) and for each pulse a matched filtering operation is carried out on the incoming delayed and Doppler-shifted pulse echoes. The collected data is presumed to be coherent and a range-Doppler map may be formed by executing a Fourier transform with respect to slow-time. Sophisticated array based multifunction radars are though able to electronically alter the beam direction and may revisit areas of interests multiple times thus ending up with several independent blocks of coherent data. In other applications, in order to confuse a jammer a radar may decide to alter the waveforms from time to time and similarly end up with distinctive blocks of data. The data within each block is accordingly coherent, however, the different blocks may not necessarily be coherent with each others. In order to make most out of available data, techniques are required to transform incoherent blocks into a single set of fully coherent sequence. A larger collection of coherent data will in turn permit generation of higher resolution plots which are fundamental for detection and classification [1].

There is a great deal of available literature on compressed sensing (CS) and reconstruction techniques in a radar framework [2], [3], [4]. Much of the work is related to irregular data collection and an on-following optimization. In e.g. [5] a method was proposed to sample data irregularly in slow-time domain and interpolation of any gaps. However, only a single dwell consisting of coherent data was considered. Another familiar trait of the previous works is that the sparse solution found is regarded as the final output which therefore contains a very large number of zero values. To improve upon sparse solutions a hybrid sparse reconstruction technique is suggested where the recovered sparse solution is only employed partly to fill in empty data gaps.

The overall contributions of this paper are linked with the introduction of a co-joined phase optimization and sparse reconstruction technique to transform several sets of data into a single coherent sequence. Data collected from an experimental radar setup is used for validation.

II. Radar and system model

A standard pulse-Doppler radar is assumed where transmission and reception of pulses takes place within a CPI aimed at a specific direction. After the CPI, the radar may digitally change the direction to transmit other beams and start a new CPI. Taking advantage of electronically steering arrays, the radar may at a later point decide to revisit the previous direction and collect a new dwell of data. It may also return to past regions with different waveforms and vary the length of CPIs in order to distract a jammer. It is presumed that the radar acquires a total of two such CPI blocks for the same direction each block containing, respectively, N_1 and N_2 number of pulses. The incoming signal can be characterized by

$$s(t, u_b) = \sum_n \sigma_n p(t - \Delta_n) e^{j v_{n,u_b}} + \tilde{w}(t), \tag{1}$$

where u_b, $b = 1, 2$ indicates slow-time with respect to the first or second CPI, $u_1 = 1, ...N_1$ and $u_2 = 1, ...N_2$. t is fast-time, σ_n are the reflectivity levels of incoming echoes while Δ_n is the signal delay of each reflector n and $j = \sqrt{-1}$. $\tilde{w}(t)$ is white Gaussian noise and $e^{j v_{n,u_b}}$ is the Doppler phase shift which for fixed velocity targets is modeled by

$$v_{n,u_b} = v_{n,u_b-1} + \frac{4\pi f_c \theta_n}{c\,\mathrm{PRF}}, \tag{2}$$

where θ_n is the radial velocity of target n, f_c being the carrier frequency, PRF is the pulse repetition frequency and c is the speed of light [6]. For convenience we define $v_{n,0} = 0$. After emission of each waveform $p(t)$ the radar samples any incoming pulse reflections and a pulse compression operation is carried out via the time-reversed and conjugated $p^*(-t)$,

$$Y_b(t, u_b) = \sum_n \sigma_n p^*(-t) * p(t - \Delta_n) e^{j v_{n,u_b}} + w(t) \tag{3}$$

Dette er en postprint-versjon / This is a postprint version.
DOI til publisert versjon / DOI to published version: 10.1109/RADAR.2017.7944194

where $*$ designates convolution in fast-time. The fast-time parameter will normally also be discrete, re-writing this with regard to the CPI and with range bins as the first parameter we arrive to

$$\mathbf{Y}_b(r, u_b) = Y(r\ \Delta t, u_b)\ \in \mathbb{C}^{N_b \times R},\ r = 1, 2, ..., R, \quad (4)$$

given Δt as the time-resolution of the radar. $R\Delta t$ thus corresponds to the largest time-delay associated with the maximum unambiguous radar range. The total number of transmitted and received pulses over the two blocks is

$$N = N_1 + N_2. \quad (5)$$

Within these N pulses we can safely assume that the targets only vary slightly in amplitude and there is no range walk or it has already been compensated for. The two-block aggregated data is represented by

$$\mathbf{Y}(r, u) = [\mathbf{Y}_1(r, u_1)\ \mathbf{Y}_2(r, u_2)]\ \in \mathbb{C}^{N \times R}, \quad (6)$$

given $u = 1, 2, ..., N$. For further processing each slow-time vector of $\mathbf{Y}(r, u)$, $\mathbf{y}_r(u)$, is conventionally multiplied by a window tapering function $\mathbf{w}(u)\ \in \mathbb{C}^{N \times 1}$. Performing a Fourier transformation yields the Doppler profile $\mathbf{d}_r(\omega)$ for range bin r:

$$\mathbf{d}_r(\omega) = \mathbf{F}\ \mathbf{w}(u)\mathbf{y}_r(u)\ \in \mathbb{C}^{N \times 1}. \quad (7)$$

$\mathbf{F}$ is the discrete Fourier matrix of size $N \times N$, $\mathbf{F}_{k,l} = \exp(-2\pi jkl/N)$. Clustering together the profiles over all ranges gives a range-Doppler $\mathbf{D}(r, \omega)$ representation of radar data. The main factors forming the contours in a Doppler profile are constant phase variations originating from (2). Targets showing a consistent velocity will after Fourier processing appear contracted in Doppler as long as the data is sufficiently coherent. In contrast, with two incoherent blocks the target Doppler model (2) over N pulses is likely to project a more discontinuous behavior

$$v_{n,u} = v_{n,u-1} + P(u)\frac{4\pi f_c \theta_n}{c\ \mathrm{PRF}}, \quad (8)$$

where any phase discrepancies are described by the function $P(u) \in \mathbb{R}$. A leap in phase will occur at starting of the second block causing incoherence and leading to Doppler leakage and declined integration gain.

A. Phase optimization and Sparse reconstruction

The presence of two independent sections in $\mathbf{Y}(r, u)$ demands appropriate processing before the data may be regarded as a single consistent entity. In order to transform the data into a coherent set appropriate phase adjustment needs to take place:

$$\tilde{\mathbf{Y}}(r, u) = [\mathbf{Y}_1\ e^{j\phi}\mathbf{Y}_2]\ \in \mathbb{C}^{N \times R}, \quad (9)$$

where ϕ attempts to reverse the incoherence. Determining the phase value can be a challenging task and herein a combined sparse reconstruction approach is introduced; assuming that each range bin contains a relative few number of targets. Utilizing a sparse reconstruction technique also offers additional leverage as a more generalized solution of this form is sought:

$$\hat{\mathbf{Y}}(r, \hat{u}) = [\mathbf{W}_A\ \ \mathbf{Y}_1\ \ e^{j\phi}\mathbf{Y}_2\ \ \mathbf{W}_B]\ \in \mathbb{C}^{L \times R}. \quad (10)$$

The sparse reconstruction solution to the posed problem is hence an attempt to assemble an expanded range-Doppler profile while simultaneously correcting for any phase discrepancies. In the extended $\hat{\mathbf{Y}}(r, \hat{u})$ reconstruction $\mathbf{W}_A(r, \dot{u}_1) \in \mathbb{C}^{N_A \times R}$ and $\mathbf{W}_B(r, \dot{u}_1)\ \in\ \mathbb{C}^{N_B \times R}$ represent extrapolated samples. For each range bin; N_A and N_B number of additional slow-time samples are extrapolated at the edges containing respectively $N_A \geq 0$ and $N_B \geq 0$ number of values. The total number of available slow-time pulses in the regenerated $\hat{\mathbf{Y}}$ comes to

$$L = N + N_A + N_B. \quad (11)$$

Additionally extrapolated samples provide extra degrees of freedom for sparse reconstruction and have potential to improve the Doppler bin resolution. The rationale being that a sparse solution to the problem must attempt to maximize the sparsity which is achieved if objects of interest are extended with a determined velocity and consequently get more and more narrowly confined to an exact velocity [5].

In the following, a column representing range bin r of the reconstructed $\hat{\mathbf{Y}}(r, \hat{u})$ is designated by $\hat{\mathbf{y}}(\hat{u})_r\ \in\ \mathbb{C}^{L \times 1}$, $\hat{u} = 1, 2, ..., L$, though the subscript is dropped for clarity. The same applies for $\tilde{\mathbf{y}}(u)$ being a column of $\tilde{\mathbf{Y}}(r, u)$. The association between the reconstructed slow-time data and its Doppler profile is given by

$$\hat{\mathbf{d}}(\hat{\omega}) = \hat{\mathbf{F}}\ \hat{\mathbf{w}}(\hat{u})\hat{\mathbf{y}}(\hat{u})\ \in \mathbb{C}^{L \times 1} \quad (12)$$

where $\hat{\mathbf{F}}$ is an $L \times L$ Fourier matrix.

Next, a binary selection matrix is defined $\mathbf{M}\ \in\ \mathbb{B}^{N \times L}$ by taking an $L \times L$ identity matrix $\mathbf{I}_{L \times L}$ and removing the first N_A and the last N_B rows. The selection matrix is to allow for extraction of values from slow-time positions with acquired data. The tapering function $\bar{\mathbf{w}}(u)$ is constructed by selecting a windowing function of L entries, $\hat{\mathbf{w}}(\hat{u}) \in \mathbb{C}^{L \times 1}$, and truncating it: $\bar{\mathbf{w}}(u) = \mathbf{M}\hat{\mathbf{w}}(\hat{u})\ \in \mathbb{C}^{N \times 1}$.

Several techniques may be adopted to solve the stated problem. A direct descriptive approach in order to simultaneously optimize the phases and establish a sparse solution can be based on splitting the problems into two parts, an inner sparse reconstruction and an outer phase optimization.

1) The inner algorithm, assumes the phase ϕ is provided and finds a sparse Doppler profile $\hat{\mathbf{d}}(\hat{\omega})$ consisting of L Doppler samples while concurring with the observations where available. This requirement of a profile being in agreement with measured data can, be expressed as

$$(\mathbf{M}\hat{\mathbf{y}})(u) = \tilde{\mathbf{y}}(u). \quad (13)$$

For clarity, the index terms are only given for the final product. With windowing functions incorporated the requirement

Dette er en postprint-versjon / This is a postprint version.
DOI til publisert versjon / DOI to published version: 10.1109/RADAR.2017.7944194

becomes

$$\mathbf{M}(\hat{\mathbf{w}}\hat{\mathbf{y}})\ (u) = (\mathbf{M}\hat{\mathbf{w}})\tilde{\mathbf{y}}\ (u), \tag{14}$$

$$\text{or} \qquad \hat{\mathbf{F}}_M\hat{\mathbf{d}}\ (\hat{\omega}) = \bar{\mathbf{w}}\tilde{\mathbf{y}}\ (u), \tag{15}$$

where $\hat{\mathbf{F}}_M$ is the partial inverse Fourier matrix $\hat{\mathbf{F}}_M = \mathbf{M}\hat{\mathbf{F}}^* \in \mathbb{C}^{N\times L}$.

Sparse reconstruction, under convex relaxation, can therefore be detailed by

$$\hat{\mathbf{d}}(\hat{\omega}) = \arg\min ||\dot{\mathbf{d}}(\hat{\omega})||_1 \tag{16}$$

$$s.t. \quad || \hat{\mathbf{F}}_M\ \dot{\mathbf{d}}(\hat{\omega}) - \bar{\mathbf{w}}(u)\ \tilde{\mathbf{y}}(u)\ ||_2 \leq \varepsilon \tag{17}$$

where ε is acceptable error.

2) The outer algorithm addresses phase optimization by recovering

$$\hat{\phi} = \arg\min_{\phi} ||\hat{\mathbf{d}}(\hat{\omega})||_1 \tag{18}$$

such that the same L_1 norm is minimized. In the most basic form, the outer algorithm searches over ϕ, correcting for the phase shift in $\tilde{\mathbf{y}}(u)$, and for each iteration the inner algorithm resolves the sparse Doppler problem.

Collecting solutions across all ranges $r = 1, 2, ..., R$ gives a full range-Doppler map matrix $\hat{\mathbf{D}}(r, \hat{\omega}) \in \mathbb{C}^{L\times R}$ with any extrapolated values. Notice that this process is independent for each range bin and may be executed in parallel. For the outer loop any standard nonlinear programming solver may be applied; however, several efficient algorithms have been proposed in the literature with regard to optimization and sparse reconstruction [7], [6], [8], [9] and we refer to them for more details. We remark that to reduce computational complexity the phase optimization process may be carried out only once, or alternatively over a representative set of range bins.

B. Hybrid reconstruction

A disadvantage with a sparse solution is that it can be viewed as performing a threshold based detection. A low value for ε will preserve noise in the optimization process thus not yielding clear fixation with respect to targets; while selecting larger threshold values can make more sensitive targets disappear. A merger of the sparse solution with real data is therefore examined next. At corresponding slow-time blocks without any radar measurements results from the sparse solution are utilized otherwise the original data, after phase corrections with the obtained ϕ is retained; or alternatively linearly combined with the sparse solution.

The hybrid range-Doppler map is constructed by transforming the sparse range-Doppler solution back to time domain

$$\hat{\mathbf{Y}}_S(r, \hat{u}) = \hat{\mathbf{F}}^*\hat{\mathbf{D}}(r, \hat{\omega}) \in \mathbb{C}^{L\times R} \tag{19}$$

which is then merged with available measurements after tapering and phase shifting

$$\mathbf{Y}_{Hyb}\ (r, \hat{u}) = \begin{cases} \alpha\bar{\mathbf{w}}\tilde{\mathbf{Y}}(r, \hat{u}) + \sqrt{(1-\alpha^2)}\hat{\mathbf{Y}}_S(r, \hat{u}), & N_A < \hat{u} \leq N_A + N \\ \hat{\mathbf{Y}}_S(r, \hat{u}), & \hat{u} \leq N_A,\ \hat{u} > N + N_A \end{cases} \tag{20}$$

where $\hat{\mathbf{F}}^* \in \mathbb{C}^{L\times L}$ is the inverse Fourier matrix and $0 \leq \alpha \leq 1$. A Fourier transform across slow-time forms the final hybrid range-Doppler map:

$$\mathbf{R}_{Hyb}\ (r, \hat{\omega}) = \hat{\mathbf{F}}\ \mathbf{Y}_{Hyb}\ (r, \hat{u}) \in \mathbb{C}^{L\times R}. \tag{21}$$

α may be chosen to scale the solutions appropriately. For detection purposes more emphasis may be placed on the sparse solution, i.e. α close to zero. To preserve the more subtle details all of the original (phase shifted) data can be kept in place by setting α to greater values.

III. Experiments

To evaluate the performance of the proposed methods data acquired from an experimental FFI radar. The S-band radar was aimed at a commercial Boeing 737-800 flying at a distance of 6.2km. The system was operating at 3.3 GHz with a bandwidth of 50MHz, LFM pulses with horizontal polarization and PRF of 4kHz. The maximum range being approximately $R = 10$km.

Utilizing the radar, a dwell of 18 pulses was collected and figure 1 shows the idealistic range-Doppler map assuming all pulses are fully coherent. In all results the Blackman window has been applied. There is a great amount of ground clutter in the image which has willingly not been filtered out; the overall resolution from 18 pulses is clearly also not sufficient to fully isolate the aircraft. To transform this data into a more realistic case scenario the slow-time samples were divided into two blocks, one consisting of 12 pulses and the other of 6 pulses. The two sections made incoherent with each others by introducing a phase change of $\tilde{\phi} = \frac{\pi}{2}$ on the second sequence. Figure 2 displays the corresponding incoherent range-Doppler map where both the clutter and the aircraft experience clear leakages in Doppler.

The incoherent data is used to solve the posed problem of determining the optimized phase value and to do an extrapolated sparse reconstruction over each range-bin. For the sparse algorithm $\varepsilon = 2\hat{\sigma}$ is used, i.e. twice the estimated noise level, alongside $N_A = N_B = 10$ yielding 20 extra extrapolated slow-time samples for each range-bin, in total giving $L = 44$ bins in Doppler. Note that with the selected low level ε a significant amount of noise is aspired retained.

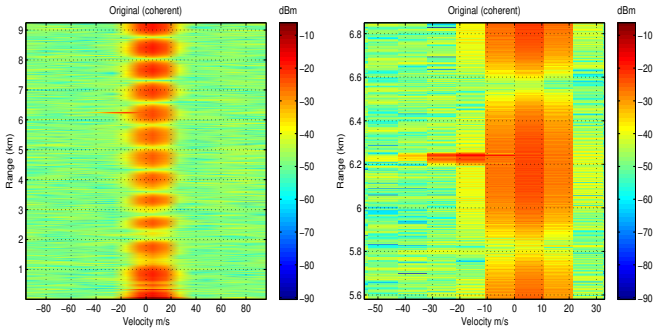

(a) Full (b) Zoomed in, PSNR=25.00dB

Fig. 1: R-D map with 18 coherent pulses

Dette er en postprint-versjon / This is a postprint version.
DOI til publisert versjon / DOI to published version: 10.1109/RADAR.2017.7944194

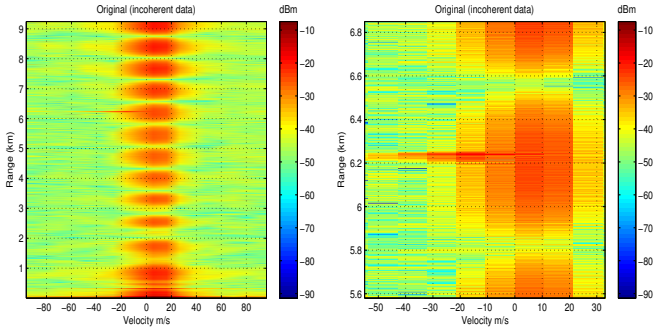

(a) Full (b) Zoomed in, PSNR=22.73dB

Fig. 2: R-D map with incoherent data blocks

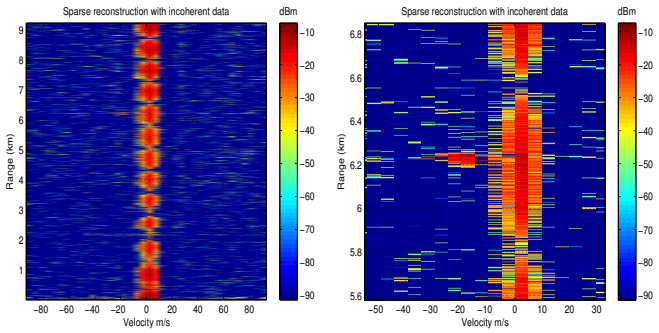

(a) Full (b) Zoomed in, PSNR=42.90dB

Fig. 3: Sparse reconstruction from incoherent data ($L = 44$)

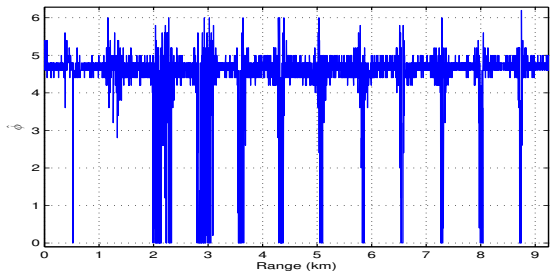

Fig. 4: Recovered phase, ($L = 44$)

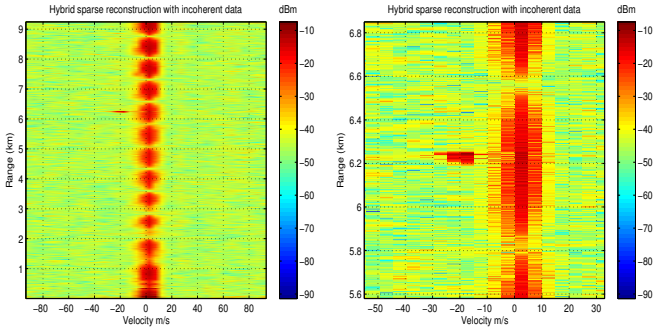

(a) Full (b) Zoomed in, PSNR=29.46dB

Fig. 5: Hybrid reconstruction from incoherent data ($L = 44$)

Figure 3 depicts the result of applying the proposed two-step technique on the incoherent data set for sparse and hybrid reconstruction. The algorithm has managed to refocus the target well and also narrowed down in Doppler to the extent that target and clutter is fully separated. The recovered phase for each range is shown in figure 4 and is in agreement with the optimal value of $\hat{\phi} = \frac{3\pi}{2}$ for stretches with the presence of either clutter, target or both. In this case, the full two-step algorithm was run over each range bin though from the plot it's evident that the phase recovered from a single typical range would also have been sufficient to provide good outcomes. Nevertheless, there is a great amount of speckle in the final sparse image coming from the low thresholding value. The hybrid solutions of section II-B tries to improve upon this by merging together the available phase corrected data and any extrapolated statistics. The result with $\alpha = 1$ is visible in figure 5 which resembles a traditionally generated range-Doppler map. The incoherent block has been compensated accordingly and the extrapolated samples increase the Doppler bin resolution to isolate out the aircraft while concurrently the collected data is exploited fully.

IV. Conclusion

Having access to longer sections of coherent data is of great importance for modern radar system as higher resolution estimates and plots can be obtained. This paper investigated a multifunction radar in this context collecting independent dwells of the same region where the various blocks may not be coherent with each others. A technique based on sparse reconstruction was proposed to compensate for phase changes and transform blocks of data into a single coherent arrangement. Sparse reconstruction additionally permits extrapolation of samples in slow-time and the paper also explored hybrid solutions constructed by merging collected and reconstructed data. The methods were tested and demonstrated on real radar data where the algorithms were shown to provide competent performance.

References

[1] A. S. Paulus, W. L. Melvin, and D. B. Williams, "Improved target detection through extended dwell time algorithm," in *IEEE Radar Conference*, 2015, pp. 484–489.

[2] M. A. Herman and T. Strohmer, "High-resolution radar via compressed sensing," *IEEE Trans. Signal Processing*, vol. 57, no. 6, pp. 2275–2284, June 2009.

[3] B. Pollock and N. A. Goodman, "Detection performance of compressively sampled radar signals," in *IEEE Radar Conference*, 2011, pp. 1117–1122.

[4] M. M. Hyder and K. Mahata, "Range-doppler imaging via sparse representation," in *IEEE Radar Conference*, 2011, pp. 486–491.

[5] J.Akhtar and K. E. Olsen, "Formation of range-doppler maps based on sparse reconstruction," *IEEE Sensors Journal*, vol. 16, no. 15, pp. 5921–5926, Aug. 2016.

[6] W. L. Melvin and J. A. S. (Eds.), *Principles of Modern Radar*. SciTech Publishing, 2013.

[7] L. C. Potter, E. Ertin, J. T. Parker, and M. Cetin, "Sparsity and compressed sensing in radar imaging," *Proceedings of the IEEE*, vol. 98, no. 6, pp. 1006–1020, 2010.

[8] M. Fornasier and H. Rauhut, *"Compressive sensing" in "Handbook of mathematical methods in imaging" O. Scherzer (Eds.)*. Springer New York, 2011.

[9] E. van den Berg and M. P. Friedlander, "Probing the pareto frontier for basis pursuit solutions," *SIAM Journal on Scientific Computing*, vol. 31, no. 2, pp. 890–912, 2008.

Dette er en postprint-versjon / This is a postprint version.
DOI til publisert versjon / DOI to published version: 10.1109/RADAR.2017.7944194